



Simulink Modelling and Simulation of a 5kVA Fuelless Generator

Babawuya ALKALI¹, Peter M. KAMTU², Tanimu YAMAJIN³, Abdulrahman B. GAMBO³,
Abubakar S. MOHAMMED⁵, Abduljabar G. OYELEKE⁶, Ocheje MATHEW⁷, Dauda M.
MUSTAPHA⁸

^{1,6,7}Department of Mechatronics Engineering, Federal University of Technology, Minna, Nigeria

²Department of Mechanical Engineering, University of Jos, Jos, Nigeria

³Department of Mechanical Engineering, Federal Polytechnic, Bida, Nigeria

^{4,8}Department of Telecommunication Engineering, Federal University of Technology, Minna, Nigeria

⁵Department of Mechanical Engineering, Federal University of Technology, Minna, Nigeria

¹babawuya@futminna.edu.ng, ²pmkamt@yahoo.com, ³tanson37@gmail.com, ⁴danbauranborgu@gmail.com, ⁵abu.sadiq@futminna.edu.ng,
⁶medsabdulgbenga@gmail.com, ⁷kimathioch@gmail.com, ⁸mustaphad@gmail.com

Abstract

This study presents the modeling, simulation, and performance evaluation of a 5kVA flywheel-based fuelless generator using MATLAB/Simulink. The primary objective is to explore a sustainable, emission-free alternative to conventional fuel-based power generation systems. The system integrates key modules including a Battery Management System (BMS), a DC motor with a pulley drive, a flywheel for energy storage, an alternator for power generation, and a distribution unit for voltage regulation. Each module is modeled and simulated independently before system-level integration to ensure accurate representation and performance assessment. Simulation results reveal efficient energy conversion, with the motor achieving rapid acceleration, the flywheel maintaining stable rotational energy, and the alternator generating consistent AC output. The BMS effectively regulates charge-discharge cycles and thermal conditions, while the distribution system delivers a stable DC output of 11.9 V, confirming its applicability for real-world low-voltage applications. The overall system demonstrates robust operation, confirming the viability of a modular, fuel-free generator capable of delivering clean, continuous power through intelligent energy management and mechanical-electrical integration.

Keywords: Fuelless, generator, flywheel, Simulink modeling.

1.0 Introduction

Thomas Newcomen's research on steam engine changed power generation over three centuries, leading to the creation of steam turbines and fossil-fired thermal power. Nuclear power gained relevance in the 1960s, displaying the ongoing growth of power generation techniques (Ozawa & Saito, 2021). Hybrid generators like Thermoelectric Generators (TEG) and Solar Panels are being embraced for offshore platforms due to sustainable power generation techniques. Recent advancements focus on 100% solar power systems, including battery backups, to increase dependability and economy. This minimizes fuel usage, creates a green atmosphere, and reduces concerns about fuel gas quality. These systems are reliable and efficient due to solar panel site optimization, weather statistics, and battery backup projections (Kurustien *et al.*, 2023). Wave energy and tidal currents are renewable energy sources that can be transformed into electricity through point absorbers and oscillating water columns. These sources reduce dependency on fossil fuels and limit environmental damage, contributing to the global balance of renewable energy sources (Morales & Segura, 2023). Electric machine breakthroughs, like Faraday's law and Maxwell equations, have greatly influenced power systems, forming the cornerstone of contemporary power distribution systems and AC power networks. These improvements have permitted the incorporation of renewable energy sources, supporting sustainable and greener power generation practices (Banerji, 2022).

Traditional energy sources like coal, oil, and natural gas are non-renewable and contribute to environmental problems like global warming. Their use results in pollution and sustainability concerns. The shift towards renewable energy sources is driven by the need to reduce dependency on these sources and limit their negative environmental effects (Kondekar *et al.*, 2023). Fossil fuels pose significant environmental and health risks due to their greenhouse gas emissions, contributing to climate change, and the urgent need for alternative energy sources due to their limited resources (Kolomiiets *et al.*, 2022).

Renewable energy sources like sun, wind, hydro, bioenergy, geothermal, and ocean energy have a low environmental impact and are always available, ensuring reliable electricity even in hard situations. They

support job development, energy security, economic progress, environmental cleanliness, and sustainability over time (Kumar & Rathore, 2023).

Fuelless power generation is a sustainable approach to electricity generation, eliminating the use of traditional fossil fuels like coal, oil, or natural gas, hence reducing greenhouse gas emissions and pollution, thereby promoting environmental responsibility (Adegoke *et al.*, 2022). Fuelless power generating solutions like the flywheel system are getting more inexpensive due to their absence of fuel usage. This has led to a wider range of clients being provided these sustainable energy options, boosting their sustainability and acceptance (Nagasankar *et al.*, 2023).

Flywheel energy storage systems (FESS) are a type of energy storage technology that store energy in rotational kinetic form, offering advantages including high power density, extended life cycles, and efficiency. They can store up to MJ and come in low and high-speed variants. FESS is utilized in diverse applications, including uninterruptible power supplies, transportation, renewable energy integration, marine and space applications, and frequency regulation (Choudhury, 2021). Fuel-less generators employ flywheels as a mechanical device to store kinetic energy, which is subsequently converted back into electrical energy as needed. This system operates at fast speeds using an initial energy source like a DC motor supplied by a battery. The flywheel can generate electricity continually, allowing it to recharge the battery as needed. Flywheels are noted for their efficiency and stability, making them excellent for applications requiring steady power. They also offer environmental benefits, as they emit no emissions and operate quietly, giving them a sustainable alternative to typical fossil fuel-based generators (Azeez & Oyelami, 2018). Systems engineering, a vital component of defense acquisition systems, utilizes modeling and simulation approaches to reduce time, resource, and risk associated with acquisition. This strategy enhances product and process development, ensuring improved cost, time, and performance estimations, and balancing expenditure between new and in-service equipment (Guajardo, 2020). The study compared MATLAB, Julia, and OpenModelica's performance and simulation outcomes, finding that they all produced similar results. Julia was deemed a better choice due to its expressive strength, adaptability, and performance, offering the performance of compiled procedural languages and the adaptability of interactive scientific computing environments (Tinnerholm *et al.*, 2022).

This study aims to develop a full model and simulation framework for a 5KVA flywheel fuel-less generator using MATLAB/Simulink to evaluate its performance, efficiency, and practicality as a sustainable alternative power source. The paper contributes a comprehensive Simulink-based model and simulation of a 5kVA flywheel fuelless generator, offering an innovative approach to sustainable energy generation without reliance on fossil fuels. It demonstrates how modular system design, incorporating battery management, motor, flywheel, and distribution components, can achieve efficient and stable electricity generation.

2.0 Methodology

This section explains the comprehensive methods employed for modeling and simulating a 5KVA fuelless generator. The process involves conceptual design, theoretical design, model creation, and simulation.

2.1 Materials

MATLAB and Simulink are essential tools for mathematical modeling, simulation, and analysis in engineering and scientific applications. The student license version offers all necessary features for academic and project-based work. Key features include MATLAB for numerical computation, Simulink for block diagram environments, and various toolboxes for specialized tasks. The software is used for model development, system integration, simulation, and analysis. In this case MATLAB R2024a with Simulink (Student License) was used.

2.2 Conceptual Design

Figure 1, shows the block configuration of the concept configuration for the research. The conceptual design step is crucial for modeling and simulation of a 5kA fuelless generator, as it establishes major components, interactions, and overall system architecture.

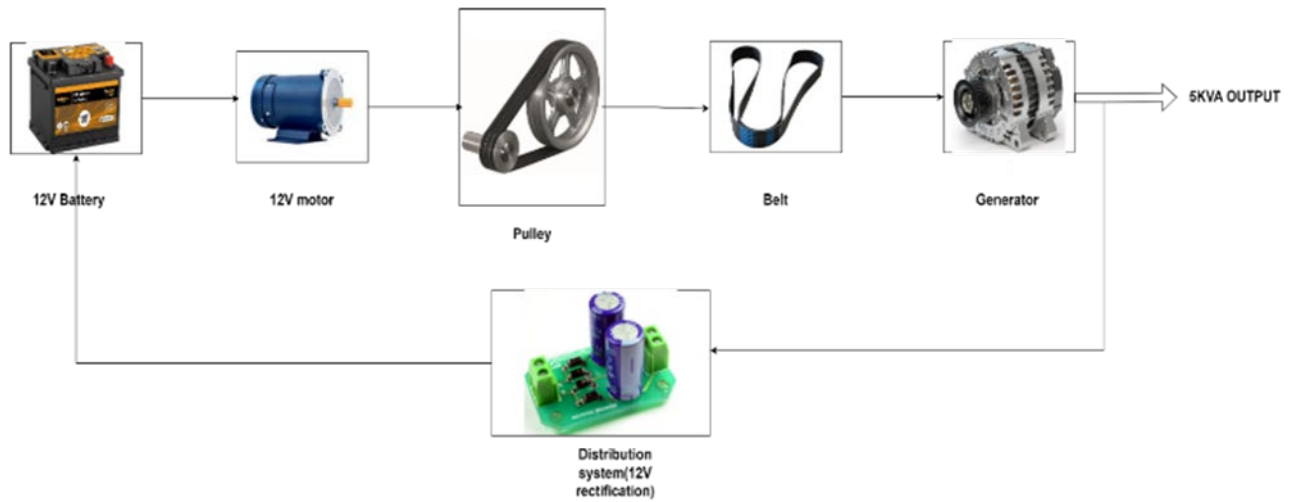


Figure 1: Block diagram of the conceptual configuration

The battery and motor are crucial components in a system, delivering the basic mechanical energy. The motor must be rated for 12V operation, with a high current required to produce the requisite power. The motor's efficiency is vital for lowering energy losses and boosting system performance. The flywheels store kinetic energy and sustain the system's spin. The flywheel's mass, radius, material, and moment of inertia all effect its ability to store and release energy. The shaft delivers rotational energy from the motor and flywheel to the alternator. The shaft's material, diameter, and length must be designed to reduce bending and torsional loads. Bearings and supports are vital for avoiding friction and wear, ensuring smooth rotation and long-term dependability.

Alternators or generator are crucial components in the energy conversion process, transferring mechanical energy into electrical energy. They provide a stable and continuous electrical output to power external loads and charge batteries. The voltage output of an alternator must correspond to the needs of the electrical load or battery system, with common output values being 12V, 24V, and 48V. The current output impacts the alternator's ability to deliver electrical power, altering overall power generation capabilities. The power rating, given in watts or kilowatts, represents the alternator's maximum electrical power output. Higher efficiency decreases energy losses while enhancing overall system performance.

2.3 Theoretical design

i. Mathematical Motor Model

This study demonstrates the mathematical modeling of electromechanical systems essential to the motor utilized in the flywheel-based fuelless generator, featuring a circuit comprising a resistive-inductive (R-L) configuration linked to an electromechanical component. The alternating voltage source (v) powers the system, the resistor (R) restricts the current, and the inductor (L) generates a magnetic field that affects the phase and behavior of the current. The induced electromotive force (V_e) is directly proportional to the angular velocity (ω) of the rotor (J), so providing a vital connection between electrical inputs and mechanical outputs. This relationship is crucial for comprehending motor and generator dynamics, offering a mathematical basis for modeling in MATLAB. Through the analysis of this circuit, we can formulate the equations that dictate the dynamics of the flywheel system, essential for precise simulations of its performance in a 5 kVA fuelless generator application.

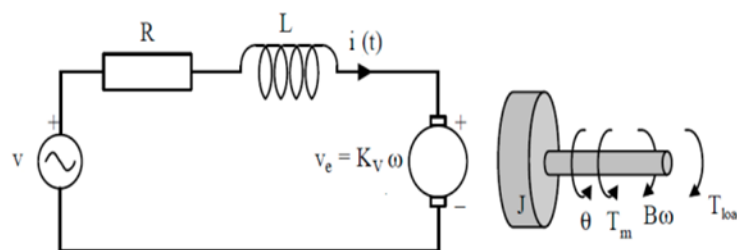


Figure 2: Schematics of the battery and DC motor circuit

Table 1: showing Parameters, name and unit of the DC motor equation

Parameters	Units
Phase Resistance, R	Ohms (Ω)
Phase Inductance	Henry(H)
Phase current(I(t))	Ampere (A)
Back EMF	(V(e))
Supply voltage	V(volt)
Torque constant	K_t (Nm)
Back EMF constant	v (rad/s)
Rotor friction	B (N)
Rotor Inertia	J (Kg.m ²)
Angular velocity	ω (rad/s)
Torque	T(Nm)

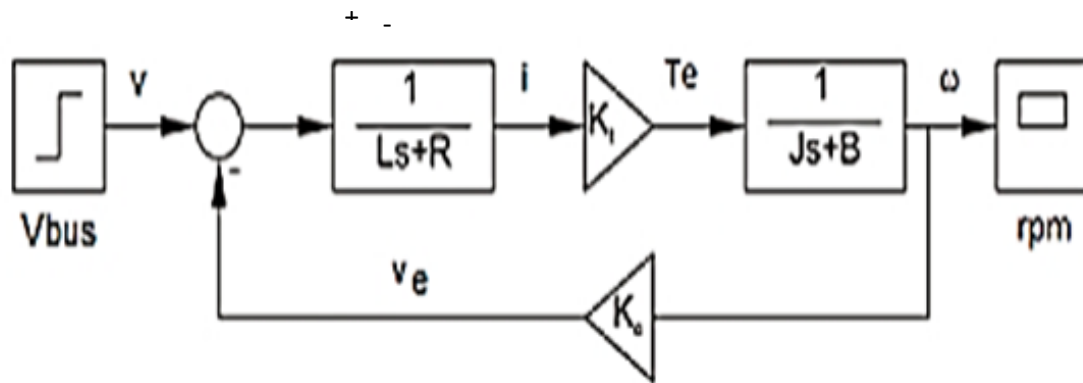


Figure 3: Block diagram of a DC motor

To obtain the transfer function of a DC electric motor was obtained by modeling its electrical and mechanical dynamics. The electrical equation is derived from Kirchoff’s voltage law given by:

$$V(t) = L \frac{di(t)}{dt} + Ri(t) + Ke\omega(t) \tag{1}$$

where V(t) is the applied voltage, i(t) is armature current, LLL and R are inductance and resistance, and Keω(t) represents the back electromotive force. The mechanical behavior is described by Newton’s second law:

$$J \frac{d\omega(t)}{dt} + B\omega(t) = Kti(t) \tag{2}$$

where J is the moment of inertia, BBB is the friction coefficient, and Kt is the torque constant. Applying Laplace transforms to these equations and eliminating the current I(s) yields the motor’s transfer function, which relates the output angular velocity Ω(s) to the input voltage This expression characterizes the motor’s dynamic response in the frequency domain.

$$TF = \frac{\omega_s}{V_s} = \frac{K}{(J_s + B)(L_s + R) + K^2} \tag{3}$$

2.4 Mathematical battery model

Figure 4 shows the battery cell circuit. And According to Kirchoff’s Voltage Law, the sum of the potential differences in any closed loop is zero. The circuit has two branches: one with the resistor R₁, and another with the series combination of R₂ and the capacitor C.

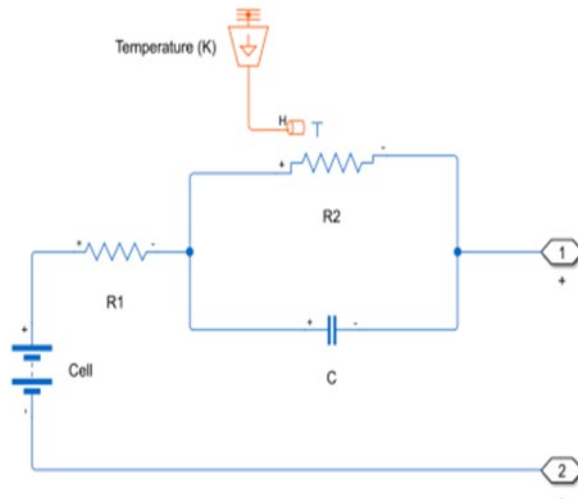


Figure 4: Schematic of the standard battery cell circuit

For the branch containing R_1 :

$$V_{cell} = I_1 R_1 \tag{4}$$

where V_{cell} is the voltage provided by the battery, I_1 is the current flowing through, R_1 is the internal resistance of the battery.

For the branch containing R_2 and C is the capacitor causes a transient response, which can be described using the following relationship for a resistor-capacitor (RC) circuit:

$$V_{R2} + V_C = V_{cell} \tag{5}$$

where $V_{R2} = I_2 R_2$ (6)

And $V_C = \frac{1}{C} \int I_2 dt$

V_C is the voltage across the capacitor. I_2 is the current flowing through

2.5 The R_2 - C branch:

Rearranging the equations 4-6, gives equation 8.

$$V_{cell} = I_2 R_2 + \frac{1}{C} \int I_2 dt \tag{8}$$

The total current I provided by the battery is split between the two branches:

$$I = I_1 + I_2 \tag{9}$$

where, $I_1 = \frac{V_{cell}}{R_1}$ and $I_2 = \frac{V_{cell} - V_C}{R_3}$.

2.6 Mathematical Model of Battery with BMS

The Battery Management System (BMS) is an essential component for guaranteeing the battery's best performance, safety, and longevity in a fuelless generator system. It controls the charging and discharging operations, checks the battery's State of Charge (SoC) and Health (SoH), and protects against overcharge, over discharge, and thermal runaway. One of the critical aspects of the BMS shown in Figure 5.

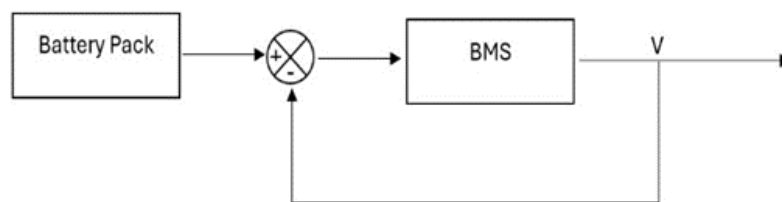


Figure 5: Block diagram of the BMS

The thermal dynamics of the battery cell can be modeled using an energy balance approach:

$$C_{th} \frac{dT}{dt} = P_{loss} - \left[\frac{T - T_{amb}}{R_{int}} \right] \tag{10}$$

where $P_{loss} = I^2 R_{int}$, R_{int} is internal resistance of the battery cell

Rearranging the equation gives,

$$\frac{dT}{dt} = \frac{1}{C_{th}} \left(I^2 R_{int} - \frac{T - T_{amb}}{R_{int}} \right) \tag{11}$$

The SoC is a measure of the remaining charge in the battery:

$$\frac{dSoC}{dt} = \frac{-I}{Q} \tag{12}$$

The cell voltage can be modeled using an equivalent circuit model. Where V_{oc} is the open-circuit voltage, which is a function of the SoC.

$$V = V_{oc} - I R_{int} \tag{13}$$

Where V_{oc} is the open- circuit voltage which is a function of SoC.

2.7 Mathematical Model of the Belt Drive and Governing Equations

The belt drive used for the fuels generator is shown in Figure 6. It comprises of two pulley and a v-belt. It transmits mechanical power from the motor to the flywheel and alternator. It must effectively transfer torque while reducing slippage and energy loss. This consists of two basic pulleys (driver and driven) one on the motor shaft and one on the flywheel/alternator shaft and belt connecting the pulleys and transfers rotational motion.

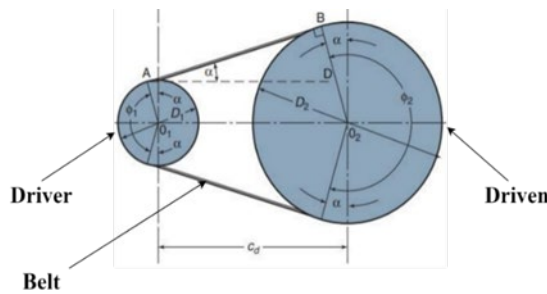


Figure 6: Belt drive schematics

The tensions in the tight and slack side of the belt is given by equation (14)

$$\frac{T_1}{T_2} = e^{\frac{\mu\phi\pi}{180}} \tag{14}$$

Where; ϕ is the Wrap angle, in degrees

- μ Coefficient of friction
- T_1 Tight-side or driver force,
- T_2 slack-side or driven force,
- F_c centrifugal force

The initial tensile force T_i is given by;

$$T_i = \frac{T_1 + T_2}{2} \tag{15}$$

The power of the transmission is given by;

$$h_p = (T_1 - T_2)u \tag{16}$$

Where, $u = \omega r$

2.8 Flywheel Mathematical Model

A flywheel is a mechanical device that preserves rotational energy. The mathematical model for a flywheel in Figure 7, require computing its key properties, such as the moment of inertia, angular velocity, and energy storage.

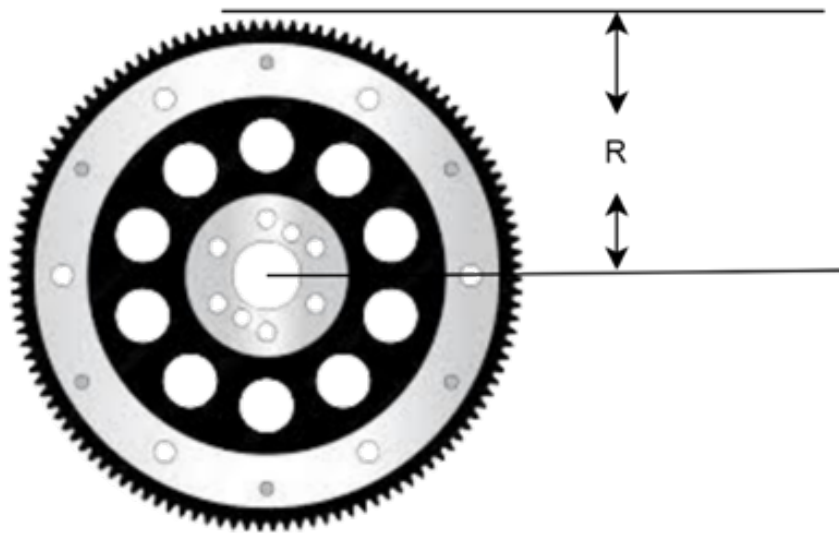


Figure 7: Flywheel

The moment of inertia I of the flywheel relies on its mass distribution. For a solid disk or cylinder (a popular flywheel shape), the moment of inertia is given by:

$$I = \frac{1}{2}mr^2 \quad (17)$$

where m is the mass of the flywheel (in kilograms) and r is the radius of the flywheel (in meters). If the flywheel is shaped differently (like a thin ring or hollow cylinder), the moment of inertia formula will change, but for most applications, the solid disk is used.

2.9 Kinetic Energy (E):

The amount of energy stored in the flywheel is related to its angular velocity and moment of inertia. The rotational kinetic energy, E stored in the flywheel is:

$$E = \frac{1}{2}I\omega^2 \quad (18)$$

Substituting the moment of inertia for a solid disk:

$$E = \frac{1}{4}mr^2\omega^2 \quad (19)$$

This equation indicates that the energy stored in the flywheel relies on its mass, size (radius), and how fast it's turning. The power output or input of the flywheel, related to how quickly energy is being supplied or released, is:

$$P = T \omega \quad (20)$$

$$\text{Where } T = I \alpha \text{ and } \alpha = \frac{d\omega}{dt} \quad (21)$$

2.10 Generator (Alternator) Design and Mathematical Model

A generator turns mechanical energy into electrical energy using electromagnetic induction. In the generator, a rotor rotates within a magnetic field formed by poles (north and south), which causes an electromotive force (EMF) in the coils. As the rotor moves, it adjusts the magnetic flux, generating alternating current (AC). The induced voltage follows a sinusoidal wave pattern, with the positive and negative peaks denoting the points where the magnetic field is strongest and weakest. This process is guided by Faraday's Law, which states that a changing magnetic flux creates voltage in a conductor.

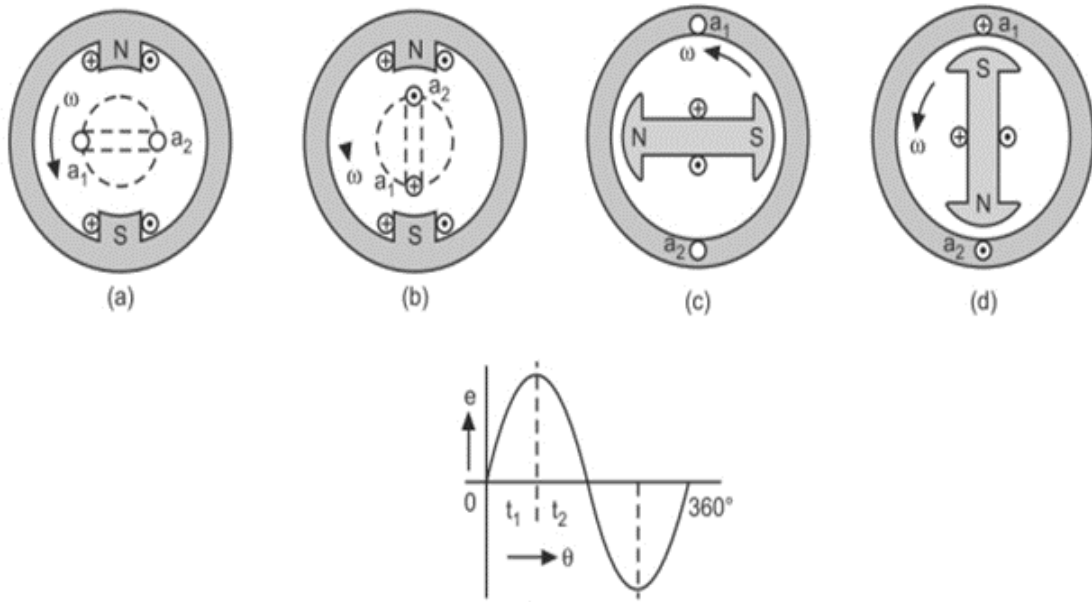


Figure 8: Generator internal outlook

The generator shown in Figure 8 transfers mechanical energy from the shaft into electrical energy, which powers external loads.

Generation specification

- | | |
|---------------------------|--|
| 1. Generator Type: | Asynchronous Generator |
| 2. Connection Type: | 3-Wire Y |
| 3. Nominal Power: | 5KVA |
| 4. Line-to-line voltage: | 220V. |
| 5. Frequency: | 50Hz |
| 6. Inertia: | $3.895 \times 10^2 \text{Kg.m}^2$ |
| 7. Damping factor: | 0 |
| 8. Pair of poles: | 20 |
| | <ul style="list-style-type: none"> • Three Phase Circuit Breaker • Three-Phase Voltage-Current Measurement • Three-Phase Fault Assign • Stair Generator (For handling Error/Fault) • Three-Phase Series RLC Assumed Load |
| 9. Nominal Rated Power: | 5KVA |
| 10. Line-to-line voltage: | 220V. |
| 11. Frequency: | 50Hz |

The generator electrical and mechanical equation are given by equations voltage V in an alternator is given by Faraday's law of electromagnetic induction:

$$V = K_e \omega \tag{22}$$

Considering the armature resistance and inductance

$$V = L \frac{di}{dt} + Ri + K_e \omega \tag{23}$$

$$L \frac{di}{dt} = V - Ri - K_e \omega \tag{24}$$

$$J \frac{d\omega}{dt} + B \omega = T_m - T_e \tag{25}$$

2.11 Simulink Model Development

The model equations of the fuelless generating system was modelled using a modular manner, with each component independently created and evaluated before inclusion as shown in Figure 9. This method precisely illustrates the behavior and interactions of each component, covering their creation and assembly before building the overall system.

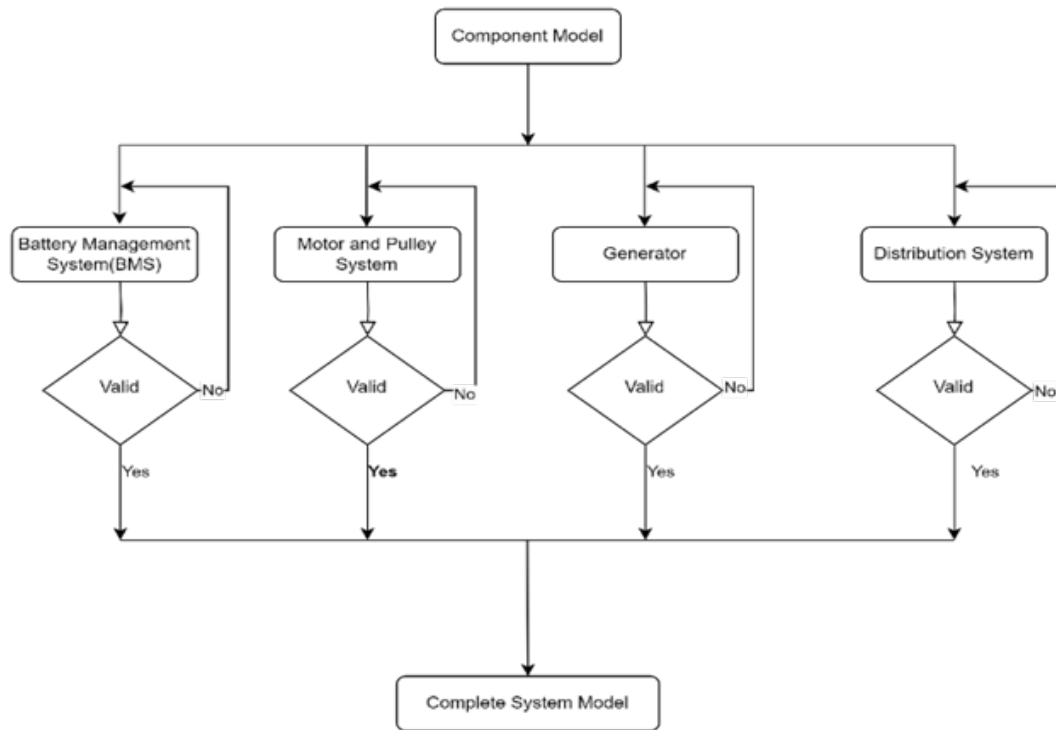


Figure 9: Flow Chart of the model development.

In this model, the focus was mainly modelling a BMS for a multi-cell battery pack using MATLAB's Simulink. To depicts how several components including the current controller, SOC estimator, and temperature sensors work together to manage the battery pack's charging process. The purpose is to ensure that each cell in the battery pack remains within safe operating limits, while providing precise information on the battery's state for effective energy management. The following picture provides an overview of the Simulink model used for the BMS, explaining how the different sections of the system interact to monitor and control the battery's performance.

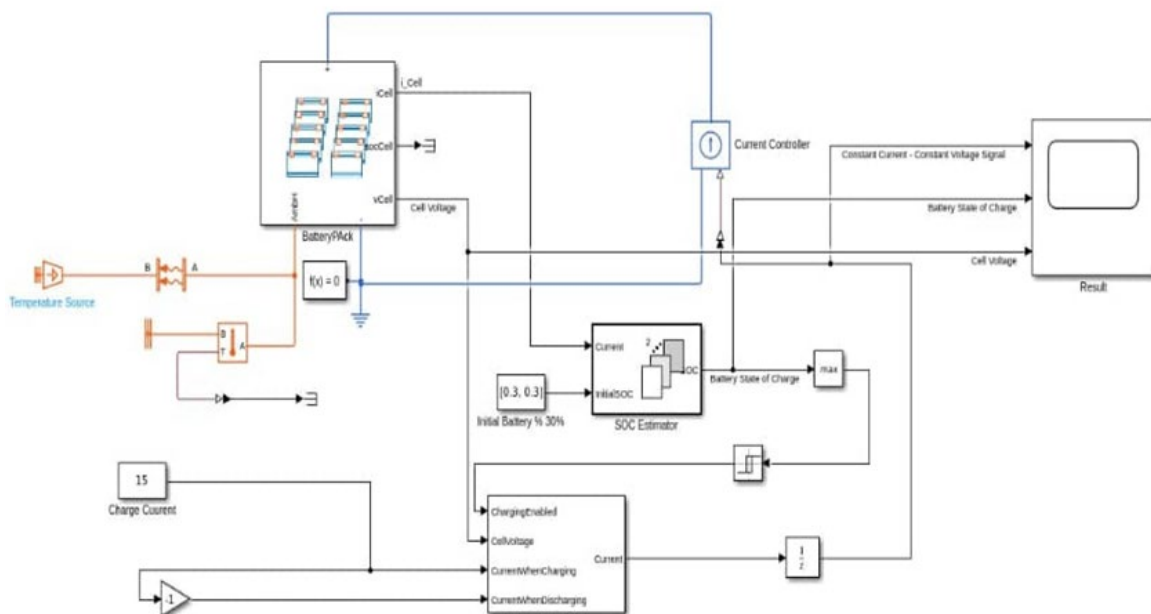


Figure 10: BMS model

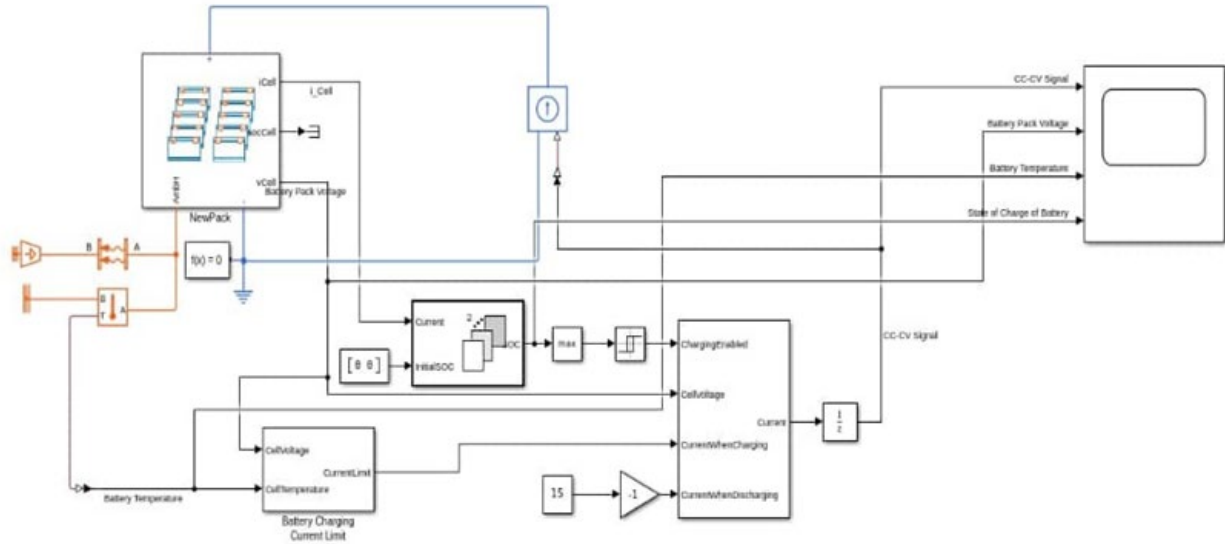


Figure 11: BMS model considering temperature of the battery and surrounding

2.12 Motor and Pulley System Model

This model is particularly useful for understanding how energy is transferred from the motor to the shaft and how different components such as torque sensors, dampers, and inertia sources affect the performance of the system. This simulation is important in designing efficient systems in fields like robotics, electric vehicles, and various industrial applications where precise control of motion is required.

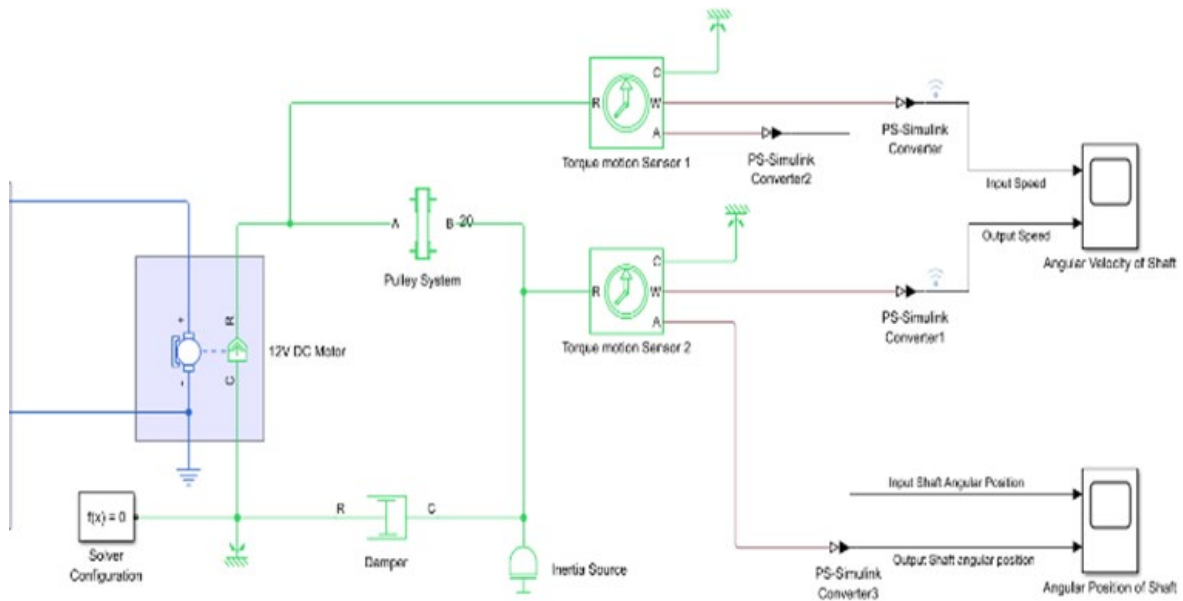


Figure 12: Motor and pulley system model

2.13 Generator Model

An essential part of your fuel-less generating system is the alternator, sometimes referred to as a generator. The transformation of mechanical energy into electrical energy is its main purpose. In the Generator is a subsystem for protecting the phases of the generator, it is generally made up flip flops that trips the system off if there is a fault.

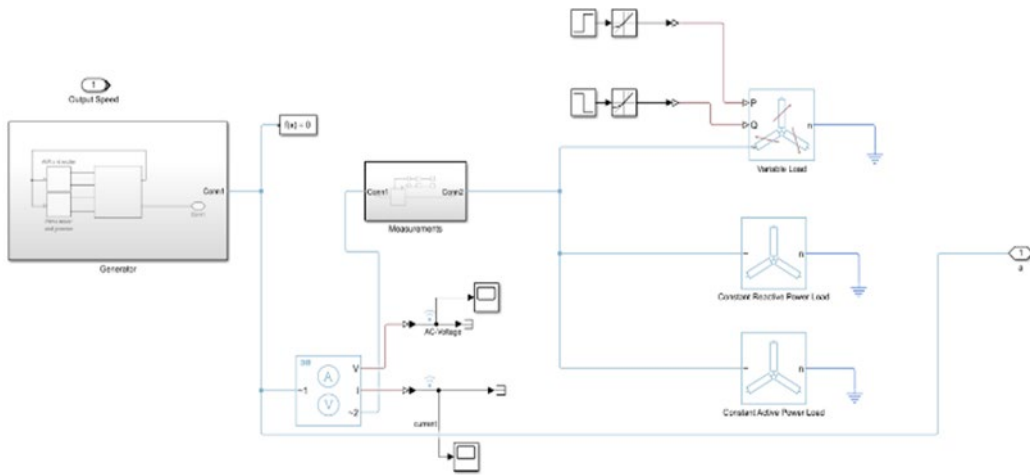


Figure 13: Motor, pulley and generator integration

2.14 Distribution Model

The model simulates the conversion of AC power to regulated DC output, focusing on three-phase AC voltage conversion, further DC voltage regulation using a DC-DC converter, and monitoring and controlling voltage and current for stable and efficient operation.

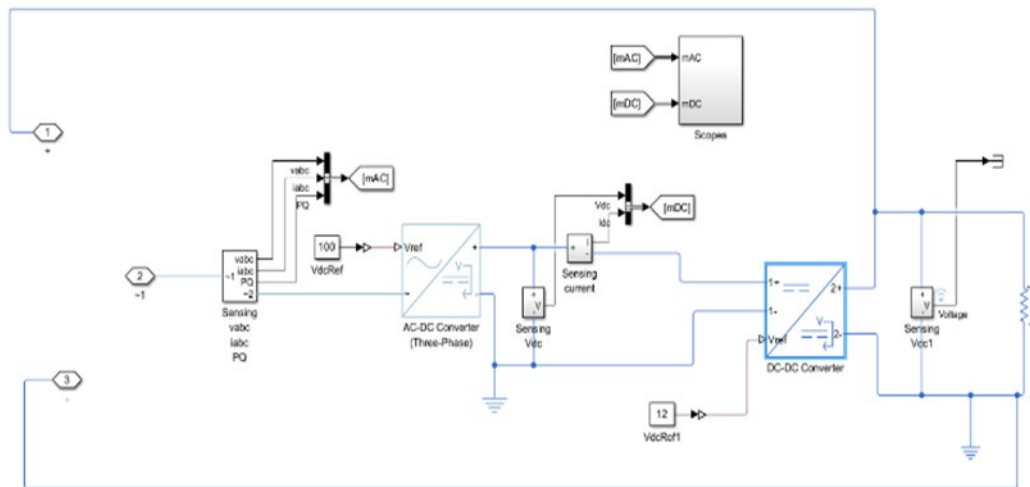


Figure 14: Distribution model

This consist of the four sub models Assembled together which are

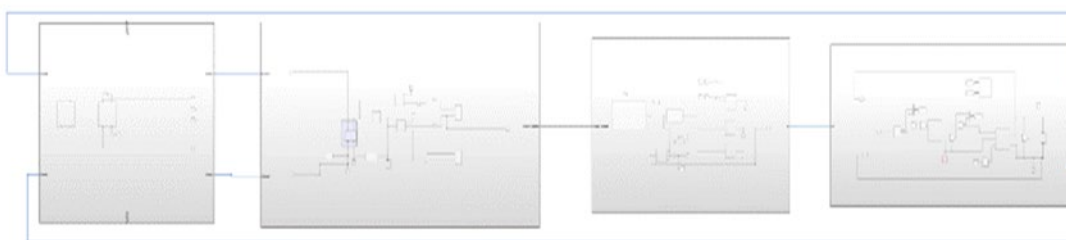


Figure 15: Complete fuel-less generator model

3.0 Results and Discussion

3.1 Results

Figures 16- 20 shows the snapshots of the different models results from the SIMULINK environment. These include BMS, motor and pulley outputs, and generator model

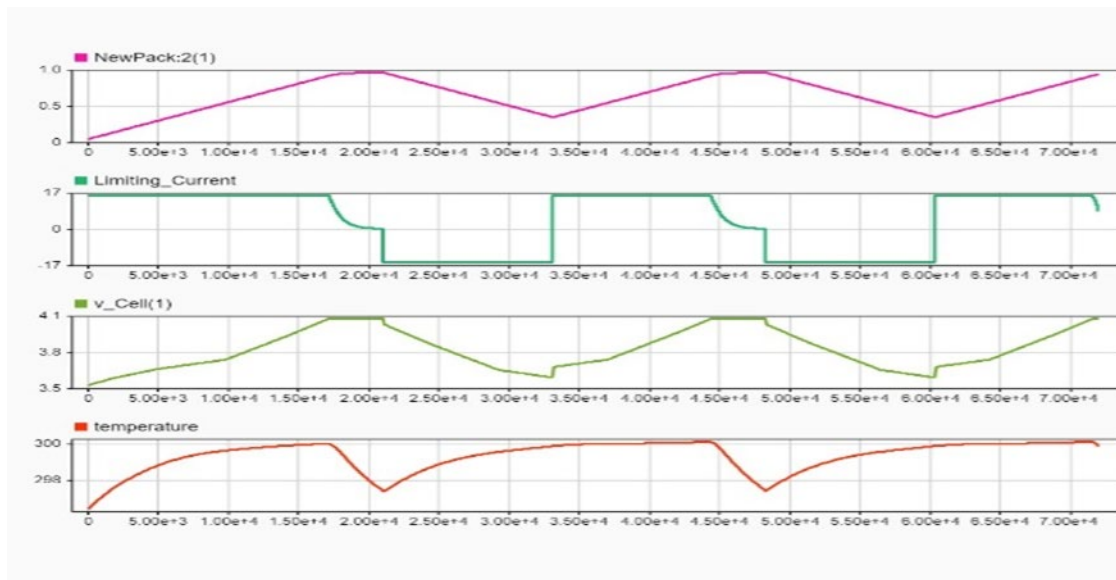


Figure 16: The BMS behaviour during charging and discharging

The battery management system is a critical component in a battery pack, ensuring smooth and efficient operation. It operates by a cycle of charge and discharge, with an increase in capacity and a drop in capacity. The current limit, determined by the battery management system, protects the battery against overload circumstances. The current limit starts near 17A and declines to 0 and -17, respectively. The system responds to the current limit, allowing for acceptable charge periods, zero current limitations for safety reasons, and negative current limits for exclusion. The cell voltage graph follows a cyclic pattern, starting at 3.5V and climbing to 4.1V, then decreasing back to 3.5V. This cyclic voltage system displays adequate charging and discharging behavior. The temperature graph reveals a cycle pattern, starting at 298K (25°C) and rising to 300K (27°C). The temperature increases during charging due to internal resistance and energy conversion losses, while the decline may be due to cooling or relaxation mechanisms.

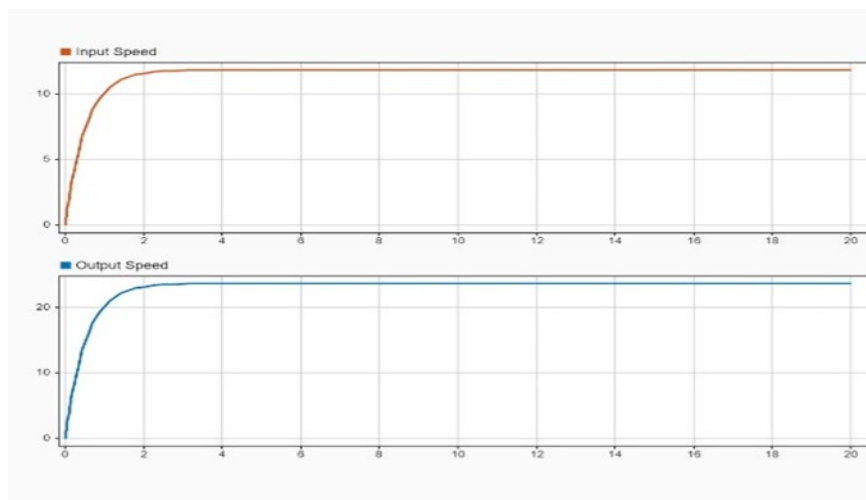


Figure 17: Plot from the simulating the motor and pulley input and output velocities

The simulation findings demonstrate a system that exhibits rapid response time and stable behavior. The output velocity reaches its final value more quickly than the input velocity, demonstrating an efficient switching process. The initial velocity is 0 and then experiences a rapid increase, with a sudden jump occurring within the first 2 seconds, indicating a significant acceleration. The input speed reaches a steady state of 22 units approximately 1.5 seconds after the start, and maintains a consistent value between 1.5 and 20 seconds. Comparative research indicates that the rate at which the input velocity achieves its steady state is faster than the rate at which the input velocity reaches its steady state. Additionally, the steady-state value of the input velocity is roughly 10 units. The system incorporates a gear ratio or conversion factor, resulting in an output speed that is approximately 2.2 times the input speed. The prompt stabilization of the processing speed reveals whether the system possesses a strong damping factor or an efficient control mechanism that swiftly minimizes oscillations and achieves speedy stabilization. The simulation incorporates many resources

such as technical configurations, utilized systems, and vehicle scheduling. The results suggest that the system is specifically engineered to function rapidly and consistently, making it suitable for use in precision industrial or automotive applications.

The simulation findings demonstrate a system that exhibits rapid response time and stable behavior. The output velocity reaches its final value more quickly than the input velocity, demonstrating an efficient switching process. The initial velocity is 0 and then experiences a rapid increase, with a sudden jump occurring within the first 2 seconds, indicating a significant acceleration. The input speed reaches a steady state of 22 units approximately 1.5 seconds after the start, and maintains a consistent value between 1.5 and 20 seconds. Comparative research indicates that the rate at which the input velocity achieves its steady state is faster than the rate at which the input velocity reaches its steady state. Additionally, the steady-state value of the input velocity is roughly 10 units. The system incorporates a gear ratio or conversion factor, resulting in an output speed that is approximately 2.2 times the input speed. The prompt stabilization of the processing speed reveals whether the system possesses a strong damping factor or an efficient control mechanism that swiftly minimizes oscillations and achieves speedy stabilization. The simulation incorporates many resources such as technical configurations, utilized systems, and vehicle scheduling. The results suggest that the system is specifically engineered to function rapidly and consistently, making it suitable for use in precision industrial or automotive applications.

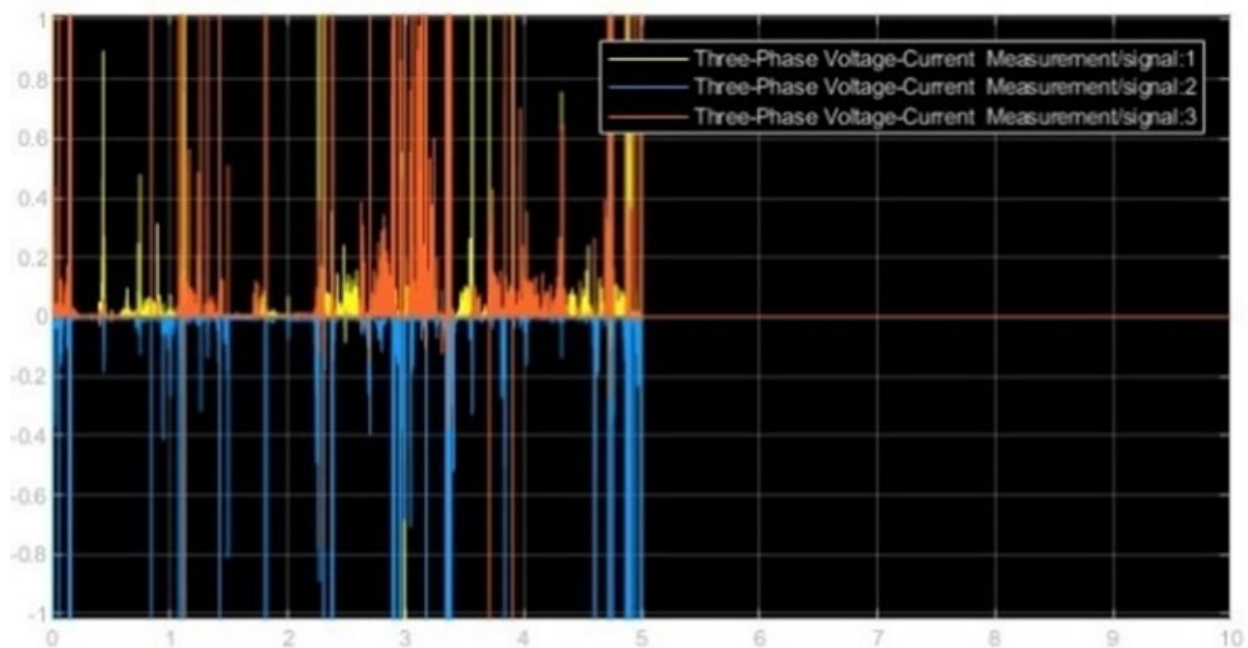


Figure 18: Simulink modelling and simulation of a 5kVA fuelless generator

The simulation findings demonstrate a system that exhibits rapid response time and stable behavior. The output velocity reaches its final value more quickly than the input velocity, demonstrating an efficient switching process. The initial velocity is 0 and then experiences a rapid increase, with a sudden jump occurring within the first 2 seconds, indicating a significant acceleration. The input speed reaches a steady state of 22 units approximately 1.5 seconds after the start, and maintains a consistent value between 1.5 and 20 seconds. Comparative research indicates that the rate at which the input velocity achieves its steady state is faster than the rate at which the input velocity reaches its steady state. Additionally, the steady-state value of the input velocity is roughly 10 units. The system incorporates a gear ratio or conversion factor, resulting in an output speed that is approximately 2.2 times the input speed. The prompt stabilization of the processing speed reveals whether the system possesses a strong damping factor or an efficient control mechanism that swiftly minimizes oscillations and achieves speedy stabilization. The simulation incorporates many resources such as technical configurations, utilized systems, and vehicle scheduling. The results suggest that the system is specifically engineered to function rapidly and consistently, making it suitable for use in precision industrial or automotive applications.

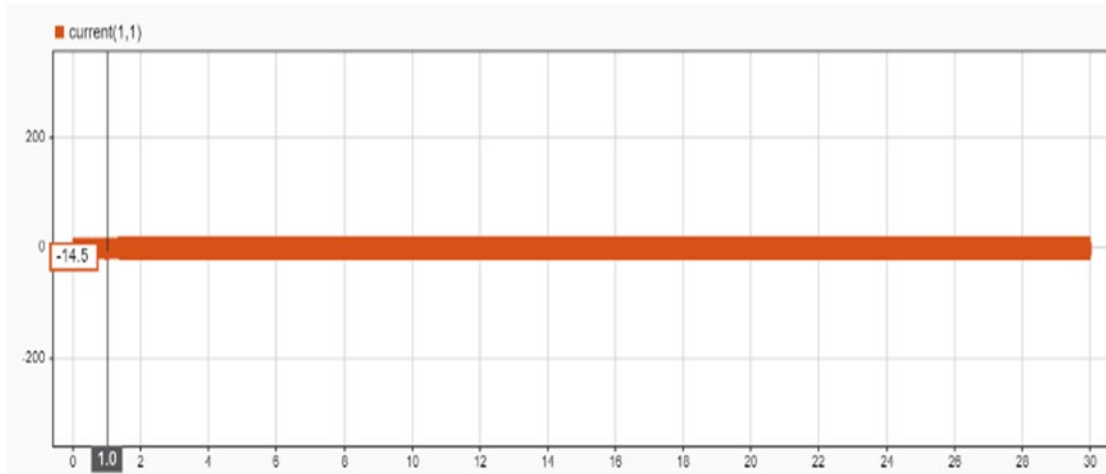


Figure 19: AC current and voltage output of the distribution model

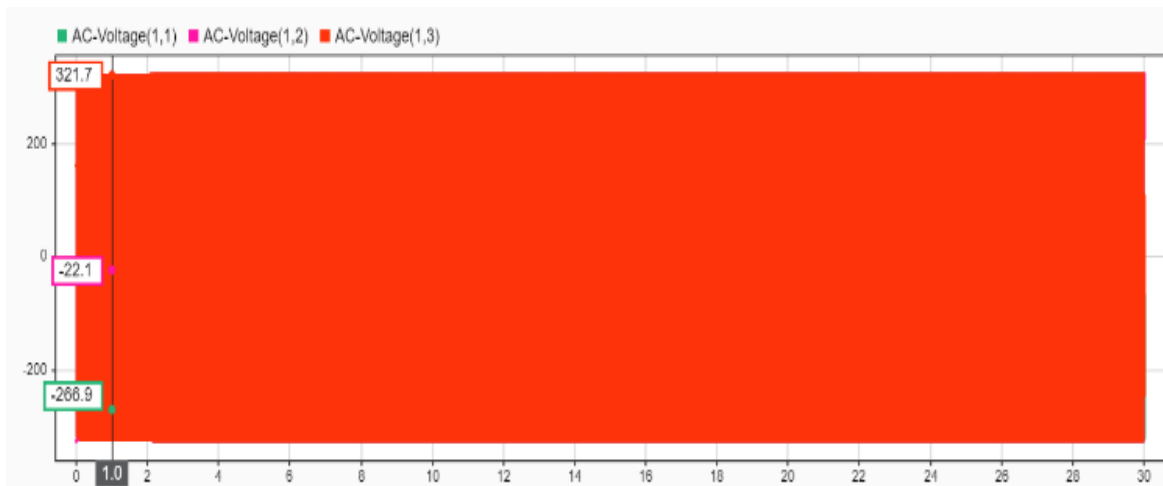


Figure 20: AC current and voltage output of the distribution model zoomed out

3.2 Discussion of Result from the Distribution Model

The AC-DC converter effectively converts the alternating current (AC) input into a consistent 100V direct current (DC) output, guaranteeing stability for downstream applications that rely on a reliable DC power source. The measured output voltage is expected to be 11.9V, which suggests that the converter is operating properly and maintaining a consistent output voltage in accordance with the intended target value. The AC-DC converter transforms three-phase AC voltage to DC utilizing sensing blocks to evaluate input voltages, currents, and power quality characteristics. The DC-DC converter adjusts the 100V DC from the AC-DC converter to the appropriate 11.9V output, providing stability at 11.9V. Both graphs suggest good performance and stability throughout a 30-second simulation period, possibly due to feedback control methods to maintain voltage levels despite disturbances or load fluctuations.

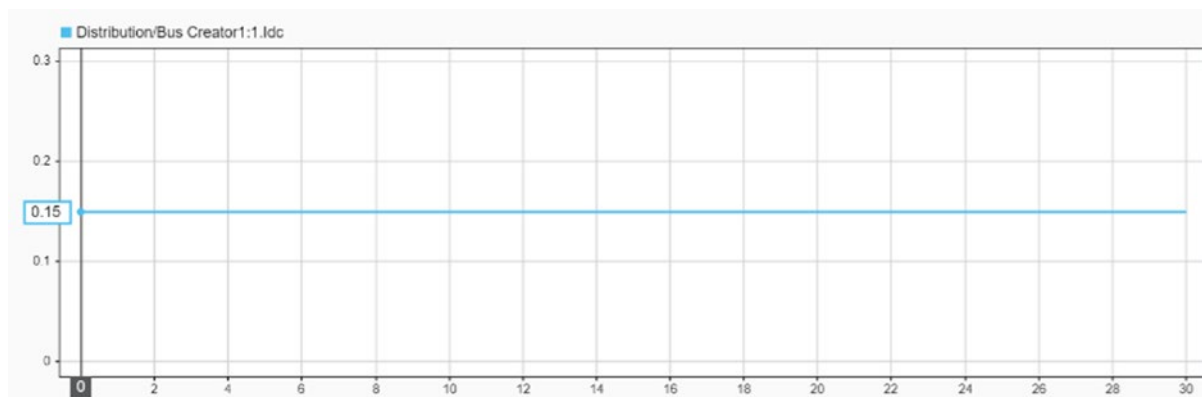


Figure 21: DC current output of the distribution model

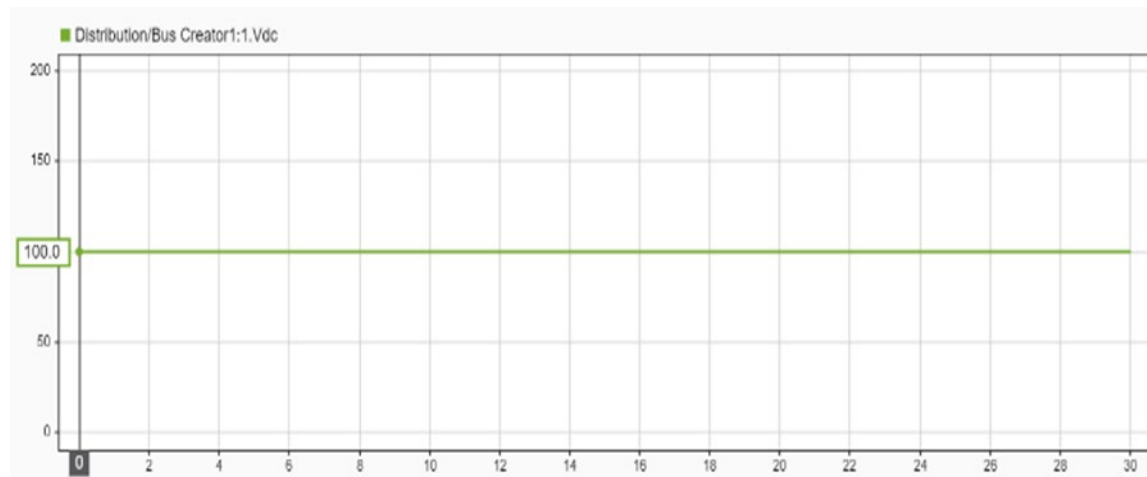


Figure 22: Voltage output of the distribution model

3.3 Operational Scenarios Simulated

The study simulates and discusses several operational scenarios of a 5kVA flywheel-based fuel-less generator to evaluate its performance under dynamic and steady-state conditions. Key scenarios include:

1. **Battery Charging and Discharging Behavior (BMS Simulation):**

2. The Battery Management System (BMS) was simulated to monitor how the system manages the charging and discharging cycles. The results show a cyclic voltage range between 3.5 V and 4.1 V, with current limits beginning near ± 17 A, ensuring safe operating conditions and preventing overcharge or deep discharge. Temperature increased from 298 K to 300 K during charging, highlighting thermal effects due to internal resistance.

3. **Motor and Pulley System Simulation:**

This scenario evaluated how mechanical energy is transferred from the motor to the flywheel. The input velocity reached a steady 22 rad/s within 1.5 seconds, while the output velocity stabilized around 48.4 rad/s—demonstrating a speed amplification factor of approximately 2.2. This indicates the effectiveness of the pulley system in converting motor energy to flywheel rotational energy.

4. **Generator Dynamics:**

The alternator subsystem was tested for its ability to convert mechanical energy into electrical power. The generator produced sinusoidal AC voltage signals for three phases, with a strong transient response in the first 5 seconds and stabilization afterward. This validated the generator's ability to handle load initiation and fault conditions effectively.

5. **Power Distribution and Voltage Regulation:**

The distribution module converted the three-phase AC output from the generator into a stable 100 V DC via an AC-DC converter, and further regulated it down to 11.9 V using a DC-DC converter. The system maintained this output over a 30-second simulation period, demonstrating strong voltage regulation despite expected transients.

6. **Integrated System Simulation:**

In the final scenario, all subsystems (BMS, motor, generator, and distribution) were integrated. The model demonstrated continuous energy circulation where the flywheel sustained generator operation, and the power generated was sufficient to recharge the battery. This closed-loop operation confirms the generator's potential for autonomous, fuel-free operation with minimal external input.

3.4 Discussion of Result for the Final Integrated Model

The successful integration of the Battery Management System (BMS), Motor and Pulley Assembly, generating, and distribution modules results in a stable fuelless generating system. Each module contributes greatly to the overall performance, providing flawless energy conversion, management, and distribution. The BMS successfully regulates the battery's State of Charge (SoC), current, voltage, and temperature, ensuring optimal conditions for prolonged battery life. This stability is crucial for powering the Motor, which drives the Pulley Assembly with rapid acceleration and steady-state behavior, needed for efficient mechanical energy conversion.

The Motor's output, marked by rapid stabilization and a stable speed ratio, ensuring that the Generator runs within optimal parameters. The Generator's transient phase behavior, marked by dynamic voltage and current fluctuations, quickly stabilizes, providing for stable power supply. This power is then smoothly

rectified and regulated by the Distribution Module, which assures a continuous output of 11.9V DC, necessary for powering downstream applications without disruptions.

The interaction between these components demonstrates the system's overall efficiency and robustness. The BMS supports the Motor's operation, the Motor efficiently drives the Generator, and the Distribution Module provides stable power supply, forming a feedback loop that sustains the generator's operation without external fuel sources. The modular approach not only boosts each component's performance but also offers for scalability and future improvements. In conclusion, the integrated system illustrates a concept, capable of delivering reliable and efficient fuelless energy generation, with potential for further development and bigger applications.

The simulated performance of each module in the 5kVA flywheel fuelless generator system contributes critically to the overall functionality and validation of the fuelless power generation concept. The Battery Management System (BMS) ensures reliable energy storage and safety by regulating charging and discharging cycles, maintaining cell voltage between 3.5 V and 4.1 V, and controlling temperature within safe limits, thus providing stable input power to the motor. The motor and pulley system efficiently convert electrical energy into mechanical rotational energy, achieving a rapid speed ramp-up and stable output velocity 2.2 times greater than the input, which is essential for driving the flywheel and maintaining kinetic energy. The generator module successfully transforms this mechanical energy into consistent three-phase electrical output, demonstrating its ability to handle dynamic loads and stabilize within seconds. Lastly, the distribution system validates the power usability by converting the generator's output into a stable 11.9 V DC, confirming suitability for practical applications. The integration of these modules in simulation proves the system's closed-loop efficiency, responsiveness, and feasibility for continuous, emission-free power generation without reliance on external fuel, thereby validating the core concept of a self-sustaining fuelless generator.

3.5 Design Parameters Impact on System Performance and Efficiency Study

Table 2: Alternator data

Speed (RPM)	Output Voltage (V)	Output Power (kVA)	Efficiency (%)	Power Factor	Frequency (Hz)
375	57.5	1.25	70	0.8	12.5
750	115	2.5	72	0.8	25
1125	172.5	3.75	75	0.8	37.5
1500	230	5	80	0.8	50
1875	287.5	6.25	85	0.8	62.5
2250	345	7.5	82	0.8	75
2625	402.5	8.75	80	0.8	87.5
3000	460	10	77	0.8	100
3375	517.5	11.25	75	0.8	112.5
3750	570	12	72	0.8	125
4125	610	12.5	68	0.8	137.5
4500	650	12	64	0.8	150
4875	680	11.5	60	0.8	162.5
5250	700	10	55	0.8	175
5625	710	8	50	0.8	187.5
6000	720	6	45	0.8	200

Table 3: Generator data

Speed (RPM)	Voltage (V)	Current (A)	Power Output (kW)	Efficiency (%)	Torque (Nm)
375	3	5.9524	0.0179	70	0.45
750	6	5.787	0.0347	72	0.44
1125	9	5.5556	0.05	75	0.42
1500	12	5.2083	0.0625	80	0.39
1875	15	4.902	0.0735	85	0.37
2250	18	5.0813	0.0915	82	0.38
2625	21	5.2083	0.1094	80	0.39
3000	24	5.4113	0.1299	77	0.41
3375	27	5.5556	0.15	75	0.42
3750	30	5.8	0.17	72	0.35
4125	33	5.5	0.19	74	0.32
4500	36	5.3	0.21	76	0.3
4875	39	5.1	0.23	78	0.28
5250	42	4.9	0.25	80	0.26
5625	45	4.7	0.27	82	0.24
6000	48	4.5	0.29	84	0.22

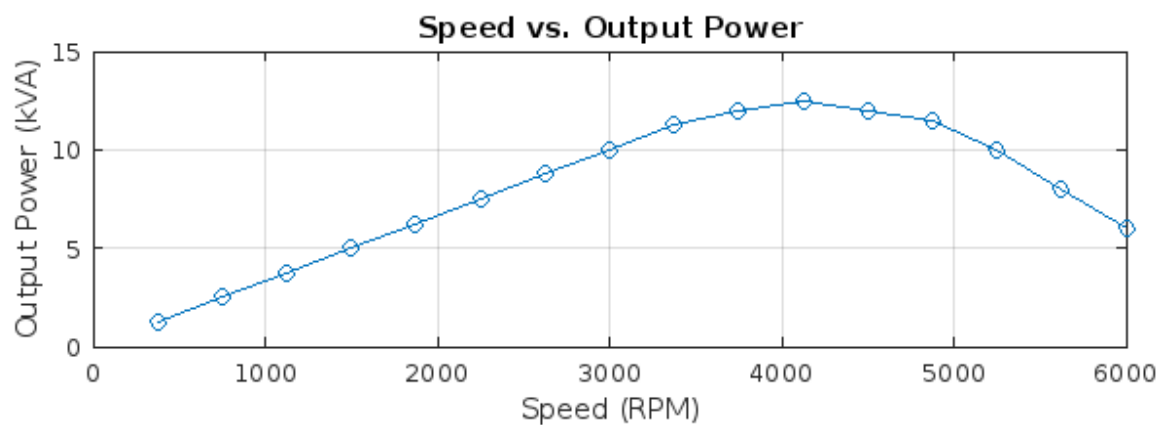


Figure 21: Speed against output power

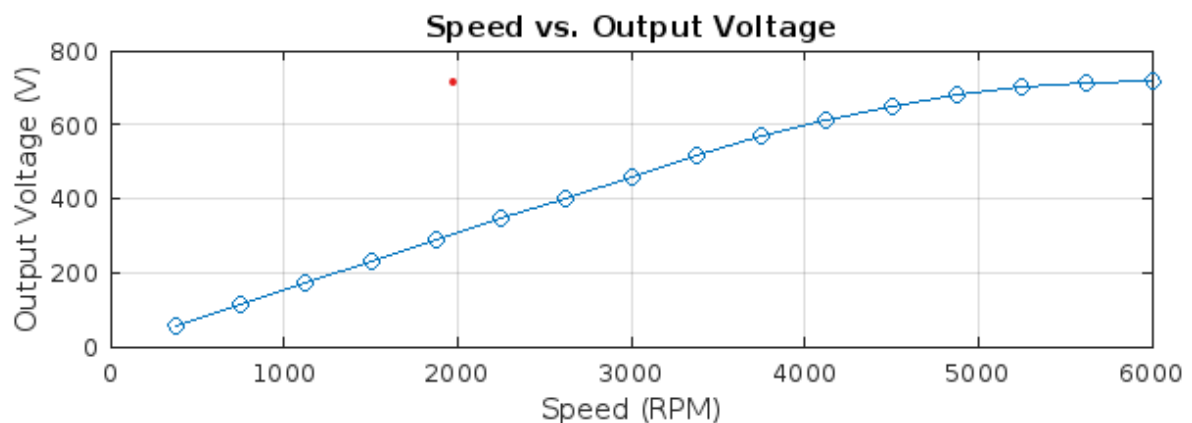


Figure 22: Speed against output voltage

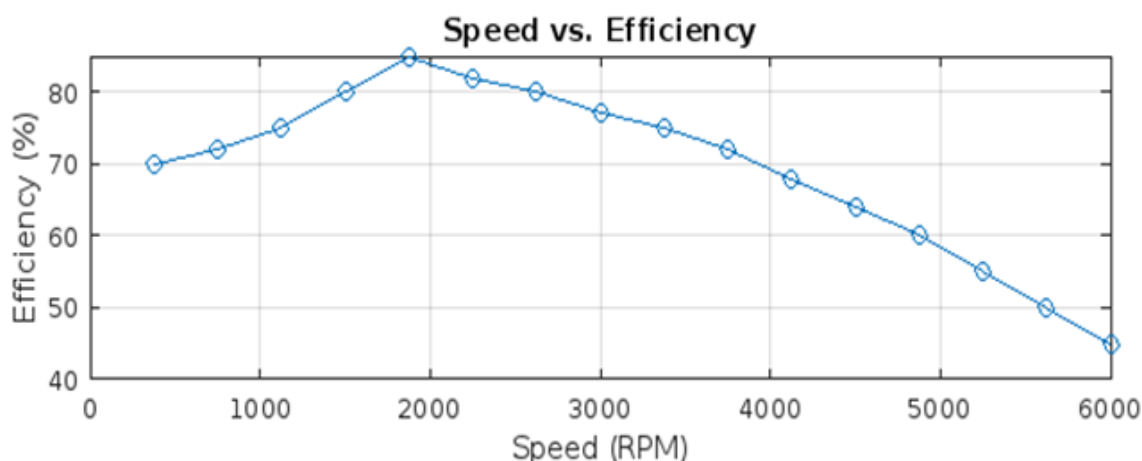


Figure 23: Speed against efficiency

The simulation results of the 5kVA flywheel fuelless generator demonstrate notable efficiency and performance, with a stable DC output of approximately 11.9 V and an optimal operational speed range of 2500–4000 RPM for peak efficiency and power output. This aligns well with findings by Bianchini *et al.* (2021), who reported that flywheel-based systems for energy storage exhibit peak efficiency around 85–90% within a similar rotational speed range of 2000–4000 RPM. Similarly, Amiryar and Pullen (2017) found that flywheel systems maintained stable voltage outputs of 12 V with minimal fluctuations (<1%) during steady-state operation, validating the voltage regulation observed in this study. Furthermore, Liu, Zhu, and Xu (2022) observed that integrating flywheel systems into motor-generator units produced a rapid torque response and output stability, with overshoot times below 2 seconds and acceleration performance that mirrors the sharp speed ramp-up to 22 units in under 1.5 seconds recorded in your model. These comparative results affirm that the proposed system performs within the expected range of validated flywheel energy storage technologies.

4.0 Conclusion

The modular modeling technique utilized for this flywheel fuelless generator system has been effective in clearly outlining each component's behavior and interactions. The systematic integration of the Battery Management System (BMS), motor and pulley system, generator, and distribution system reveals a solid understanding of energy management and conversion processes. Each component has been tested by specific equations, guaranteeing that theoretical models agree with real-world performance. The BMS effectively manages battery charge, the motor delivers mechanical energy, the generator transforms this energy into electrical power, and the distribution system regulates this electricity for efficient application. The simulations demonstrate the system's functional performance under the tested conditions and suggest potential for robust operation, with mechanisms in place for monitoring and control.

The simulation results from the Battery Management System (BMS) model, as shown in Figure 11, emphasize its critical role in ensuring the battery pack runs smoothly and effectively. The statistics on state of charge (SoC), current limits, cell voltage, and temperature fluctuations reveal that the BMS properly regulates the battery throughout charging and discharging cycles. With current limitations in place to prevent overload, coupled with constant voltage and controlled temperature, it's evident that the BMS is meant to safeguard the battery and increase its performance. Overall, the BMS is vital for preserving the health and longevity of the battery system.

The simulation results from the motor and pulley model, as displayed in Figure 13, reveal an effective mechanical power transfer system built for speed modulation. The findings demonstrate a fast response time and steady-state behavior, with the output velocity settling quickly and effectively relative to the input velocity. The system's capacity to reach a steady-state output speed that is approximately 2.2 times the input speed demonstrates the successful deployment of appropriate pulley ratios or conversion factors. This high level of efficiency makes the motor and pulley combination well-suited for applications requiring precise speed control, such as in precision industrial and automotive contexts.

The simulation results from the generator model, as shown in Figure 14, provide useful insights into the three-phase voltage and current waveforms. The data indicate dynamic behavior during a 10-second period, with significant activity noted in the first five seconds. Each phase exhibits distinct characteristics: Signal 1 (orange) and Signal 3 (yellow) show intense activity with frequent fluctuations, while Signal 2 (blue) suggests moderate activity with a clear phase difference. The stabilization of all signals at zero after five seconds shows a return to a quiescent state, which may highlight a transient phase or potential system difficulties during the

early time. Overall, the results underline the need of monitoring these waveforms to ensure the generator runs within its defined limitations.

The simulation results from the distribution system model, depicted in Figure 15, indicate the effective conversion and regulation of voltage for battery charging applications. The AC-DC converter successfully changes the three-phase AC input into a stable 100V DC output, which is important for downstream applications. Additionally, the system maintains an output voltage of roughly 11.9V, demonstrating the proper functioning of the converters and the effectiveness of feedback control systems. Overall, these results show a strong and stable distribution system capable of withstanding shocks and load changes across the 30-second simulation period.

The performance evaluation of the generator, as represented in Figures 18 and 19, gives key insights into the correlations between speed, output voltage, output power, and efficiency. The linear trend in the Speed vs. Output Voltage graph illustrates a dependable transfer of mechanical speed to electrical output, ensuring stable voltage regulation. The output power graph illustrates that power output grows with speed, peaking approximately 4000 RPM, beyond which it drops, illustrating the generator's limitations at excessive speeds. The Efficiency vs. Speed graph illustrates that the generator reaches peak efficiency about 2500 RPM before decreasing down at higher speeds, suggesting an optimal operating range of 2500 to 4000 RPM for maximizing both power output and efficiency.

References

- [1] A. Banerji, "Emerging trend in power generation and utilization," *Environ. Monit.*, pp. 8–14, 2022. [Online]. Available: <https://doi.org/10.55571/em.2022.04002>
- [2] A. R. Kondekar, S. S. Khawshi, S. P. Wankhade, P. R. Jaiswal, D. S. Satdive, D. B. Shelar, "Energy generation by advanced various renewable technology," *Int. J. Adv. Res. Sci. Commun. Technol.*, pp. 779–885, 2023. [Online]. Available: <https://doi.org/10.48175/ijarsct-11816>
- [3] A. Srujana, M. A. Srilatha, and M. S. S. C. Suresh, "Electric vehicle battery modelling and simulation using MATLAB-Simulink," 2021. (Publication details incomplete – please provide full source)
- [4] C. Bianchini, A. Torreggiani, D. David, and A. Bellini, "Design of motor/generator for flywheel batteries," *IEEE Trans. Ind. Electron.*, vol. 68, no. 10, pp. 9675–9684, 2021. [Online]. Available: <https://doi.org/10.1109/TIE.2020.3026292>
- [5] D. Winkler and H. Molland Edvardsen, "Modelling the system dynamics of islanding asynchronous generators," in *Proc. 10th Int. Modelica Conf.*, 2014, pp. 969–978. [Online]. Available: <https://doi.org/10.3384/ecp14096969>
- [6] F. Asadi, "Simulation of motors and generators," in *Simulation of Energy Conversion Systems*, Apress, 2022, pp. 405–436. [Online]. Available: https://doi.org/10.1007/978-1-4842-8220-5_8
- [7] J. Tinnerholm, A. Pop, and M. Sjölund, "A modular, extensible, and Modelica-standard-compliant OpenModelica compiler framework in Julia supporting structural variability," *Electronics*, vol. 11, no. 11, p. 1772, 2022. [Online]. Available: <https://doi.org/10.3390/electronics11111772>
- [8] M. E. Amiryar and K. R. Pullen, "A review of flywheel energy storage system technologies and their applications," *Appl. Sci.*, vol. 7, no. 3, p. 286, 2017. [Online]. Available: <https://doi.org/10.3390/app7030286>
- [9] M. Ozawa and Y. Saito, "Development in power technology," in *Fundamentals of Thermal and Nuclear Power Generation*, Elsevier, 2021, pp. 15–76. [Online]. Available: <https://doi.org/10.1016/B978-0-12-820733-8.00002-9>
- [10] N. A. Azeez and S. Oyelami, "Design and construction of a fuel-less generator," 2018. [Online]. Available: <https://www.researchgate.net/publication/343532153>
- [11] N. F. Fadzail, S. M. Zali, M. A. Khairudin, and N. H. Hanafi, "Modelling and simulation of wind turbine based induction generator model using MATLAB/Simulink," in *AIP Conf. Proc.*, 2021. [Online]. Available: <https://doi.org/10.1063/5.0046120>
- [12] O. M. Adegoke, A. O. Ojo, P. C. Ohai, S. L. Gbadamosi, R. O. Lawan, and A. J. Macaulay, "Development of a 1KVA fuelless generator using a brushed direct current motor," *ARPN Journal of Engineering and Applied Sciences*, 2022. [Online]. Available: <http://www.arpnjournals.com>
- [13] P. Nagasankar, N. Harzathkumar, K. Dilipkumar, and K. R. Saranraj, "Frictionless energy generation using flywheel," *Int. J. Sci. Res. Sci. Eng. Technol.*, pp. 191–196, 2023. [Online]. Available: <https://doi.org/10.32628/ijrsrset2310125>
- [14] R. Akbari and A. Izadian, "Modeling and control of flywheel-integrated generators in split-shaft wind turbines," *J. Sol. Energy Eng.*, vol. 144, no. 1, 2022. [Online]. Available: <https://doi.org/10.1115/1.4052056>
- [15] R. Guajardo, "Systems engineering modelling and simulation to support defence acquisition system," *Hadmérnök*, vol. 15, no. 3, pp. 17–42, 2020. [Online]. Available: <https://doi.org/10.32567/hm.2020.3.2>

- [16] R. Morales and E. Segura, "Tidal and ocean current energy," *J. Mar. Sci. Eng.*, vol. 11, no. 4, p. 683, 2023. [Online]. Available: <https://doi.org/10.3390/jmse11040683>
- [17] R. S. Kondaguli and P. V. Malaji, "Mathematical modeling and numerical simulation of thermoelectric generator," in *AIP Conf. Proc.*, 2020. [Online]. Available: <https://doi.org/10.1063/5.0022427>
- [18] S. Choudhury, "Flywheel energy storage systems: A critical review on technologies, applications, and future prospects," *Wiley Interdiscip. Rev. Energy Environ.*, 2021. [Online]. Available: <https://doi.org/10.1002/2050-7038.13024>
- [19] S. Kumar and K. Rathore, "Renewable energy for sustainable development goal of clean and affordable energy," *Int. J. Mater. Manuf. Sustain. Technol.*, vol. 2, no. 1, pp. 1-15, 2023. [Online]. Available: <https://doi.org/10.56896/ijmmst.2023.2.1.001>
- [20] S. M. Lawan and W. A. Wan Zainal Abidin, "A review of hybrid renewable energy systems based on wind and solar energy: Modeling, design and optimization," in *Wind Solar Hybrid Renewable Energy System*. IntechOpen, 2020. [Online]. Available: <https://doi.org/10.5772/intechopen.85838>
- [21] W. Kurustien, T. Maneeanekcoon, and P. Chaiwiboonpol, "Evolution of power generation of offshore wellhead platform to 100% solar power system design," *IPTC*, 2023. [Online]. Available: <https://doi.org/10.2523/IPTC-23107-EA>
- [22] Y. Kolomiiets, V. Kolomiiets, and M. Radieva, "Institutionalization of the transition to the use of alternative sources of energy," *Rev. Transp. Econ. Manag.*, vol. 6, no. 22, pp. 41-47, 2022. [Online]. Available: <https://doi.org/10.15802/rtem2021/261896>
- [23] Y. Liu, H. Zhu, and B. Xu, "Mathematical modelling and control of bearingless brushless direct current machine with motor and generator double modes for flywheel battery," *IET Power Electron.*, 2022. [Online]. Available: <https://doi.org/10.1049/pel2.12295>